communications physics

Article

https://doi.org/10.1038/s42005-025-01942-4

Experimental demonstration of complete quantum information masking and generalization of quantum secret sharing

Zhi-Feng Liu[1,2,9], Wei-Min Shang[3,4,9], Jia-Min Xu[5], Zi-Mo Cheng[1,2], Wen-Zheng Zhu[1,2], Hao Li[1,2], Pei Wan[1,2], Shu-Tian Xue[1,2], Yan-Chao Lou[1,2], Chao Chen[1,2], Zhi-Cheng Ren[1,2], He Lu[6], Fu-Lin Zhang[7] ✉, Jing-Ling Chen[4] ✉, Xi-Lin Wang[1,2,5] ✉ & Hui-Tian Wang[1,2,8]

Quantum information masking (QIM) allows encoding quantum information in multipartite systems. Complete QIM is of great significance in quantum foundation and application. However, the realization of complete QIM, even for single-qubit encoded information, is still lacking. Here, we propose to demonstrate complete QIM with 4-qubit entangled states. The proposed QIM can be readily extended to multipartite systems with arbitrary number of subsystems, enabling quantum secret sharing (QSS) and quantum teleportation between multiplayers. In experiment, we build up a 4-qubit hyperentangled state to implement complete QIM. The trace distance of 16 encoded single-qubit states falls within the range of 0.12 ± 0.02 to 0.03 ± 0.02. Furthermore, we implement QSS between six players by expanding the 4-qubit state to a 6-qubit state entangled in hybrid manner, in which we observe an average fidelity 0.85 ± 0.03 of the recovered states. Our results open the door towards QIM-enabled quantum information processing and provide applications in quantum communications.

Quantum information is a significant extension of classical information field and provides another perspective for understanding the quantum world. Many quantum information protocols have no classical counterparts, while some natural processes in classical information are forbidden in quantum cases by the so-called *no-go* theorem. A typical quantum example is quantum teleportation[1,2], in which an unknown quantum state is transferred from one place to another without physical transmission of the object itself. Quantum teleportation was prompted by the famous no-cloning principle (the first no-go theorem), which states that no physical process can perfectly duplicate any pure state[3,4]. In addition to no-cloning theorem linked to the linearity of the quantum world, there is also the no-deleting theorem[5] from the unitarity of the quantum. They are limiting that the quantum information can be neither created nor destroyed. The no-cloning theorem has an extension, the no-propagation theorem[6], which introduces the incompatibility of the local identity channels. Arising from the black-hole information paradox, the no-hiding theorem[7] proves that hiding quantum state in quantum correlations is impossible. Recently, a no-go theorem, no-masking principle[8], was found in quantum information masking (QIM). Both no-hiding theorem and no-masking principle are associated with the conservation law of quantum information. They all investigate whether the isometry exists which from original Hilbert space to bipartite Hilbert space. For the hiding case, quantum information from one of the subspaces of the bipartite Hilbert space is independent of original quantum state. While for the masking case, quantum information from any subspace is independent of original quantum state[9].

QIM provides a methodology to hide quantum information from subsystems and to spread it over the nonlocal correlation in multipartite systems. The initial information can be reconstructed from this correlation. Initially, no-masking principle[8] stipulated that quantum information pertaining to an arbitrary qubit state could not be masked in a bipartite quantum system while hidden from its subsystems. Subsequently, various studies of the maximal maskable set of quantum states[10–13] were reported. This no-masking theorem tells us that complete QIM, which enables to mask the quantum information to the maximally mixed state of an arbitrary qubit state, is impossible in a bipartite scenario. However, recent theoretical studies show that complete QIM is realizable in multipartite scenarios[8,14,15], implying that no-masking principle is significantly different from other no-go theorems. In practical experiments, QIM of a special set of qubit states

[1]National Laboratory of Solid State Microstructures, School of Physics, Nanjing University, Nanjing, China. [2]Collaborative Innovation Center of Advanced Microstructures, Nanjing, China. [3]School of Science, Tianjin Chengjian University, Tianjin, China. [4]Theoretical Physics Division, Chern Institute of Mathematics, Nankai University, Tianjin, China. [5]Hefei National Laboratory, Hefei, China. [6]School of Physics, State Key Laboratory of Crystal Materials, Shandong University, Jinan, China. [7]Department of Physics, School of Science, Tianjin University, Tianjin, China. [8]Collaborative Innovation Center of Extreme Optics, Shanxi University, Taiyuan, China. [9]These authors contributed equally: Zhi-Feng Liu, Wei-Min Shang. ✉e-mail: flzhang@tju.edu.cn; chenjl@nankai.edu.cn; xilinwang@nju.edu.cn

has been demonstrated[12,13], while achieving complete QIM for all states on the Bloch sphere remains an ongoing challenge.

More than just a no-go theorem in quantum theory, QIM is intimately connected to various quantum information processing tasks, such as quantum state identification[16], quantum bit commitment[17,18], and quantum secret sharing (QSS)[19]. And it is deeply rooted in fundamental principles such as conservation of information[20]. The primary objective of QSS is to share secret quantum information in a system involving as many participants as possible and where the full initial information must be obtained with the cooperation of multiple participants[19,21,22]. Many attempts to share information in quantum systems have been reported in the literature, such as experimental realizations of classical information[23–26] and quantum information in three-[27,28] or four-party systems[29]. However, the experimental realization of QSS with more participants is still a challenge.

Since quantum information tasks such as QSS can be seen as an expression of the versatility and scalability of QIM. Both the deepening of theoretical understanding in the realm of QIM and advancements in experimental realization have played important roles in propelling the field of QSS forward. In 2018, the proof of the unmaskability theorem provided valuable insights to help dealers choose substrates for secret sharing of classical or quantum information[8]. In 2021, the realization of photonic masking machines contributes to the proposal of QSS scheme that is independent of entanglement between receivers and is not affected by decoherence[12]. Here, we not only experimentally demonstrate complete QIM, but also implement QSS with up to six participants experimentally realistic, which is based on the extension of the most frugal case.

Results

Complete QIM

For a set of quantum states $\{|a\rangle_k\}$ in the Hilbert space H_1, a unitary operator $\mathcal{S}$ performs the mapping

$$\mathcal{S}:\bigotimes_{j=1}^{n-1}|0\rangle_j\otimes|a\rangle_k\rightarrow|\Phi\rangle_k, \tag{1}$$

where $\{|\Phi\rangle_k\}$ is in the Hilbert space $\bigotimes_{j=1}^{n}H_j$. All H_j $(j=1,\ldots,n)$ have the same dimension as H_1. If any local system H_j contains no information about $|a\rangle_k$, $\mathcal{S}$ is said to be a masker that masks quantum information in $\{|\Phi\rangle_k\}$, and this QIM process refers to complete QIM. The unitary property of $\mathcal{S}$ implies that the initial information can be extracted from $\{|\Phi\rangle_k\}$.

Here we propose complete QIM to mask an arbitrary qubit state $|\gamma\rangle_1=\alpha_0|0\rangle_1+\alpha_1|1\rangle_1$ (where the amplitudes satisfy $|\alpha_0|^2+|\alpha_1|^2=1$) in four qubits, which is the minimal number of qubits required to achieve the complete QIM for a qubit[14]. Qubits 2 and 3 are initially prepared in the Bell state of $|\varphi\rangle_{23}=\frac{1}{\sqrt{2}}(|00\rangle+|11\rangle)_{23}$. Our complete QIM is realized in three steps. First, a controlled-not (CNOT) gate $\mathcal{C}_{21}$ is operated on qubits 1 and 2 (where qubit 2 acts as the control qubit and qubit 1 is the target qubit). Then the three-qubit state becomes $|\Phi\rangle_{123}=\frac{1}{\sqrt{2}}[\alpha_0(|000\rangle+|111\rangle)+\alpha_1(|011\rangle+|100\rangle)]$. Thus, the reduced density matrix of qubit 1 is $\rho_1=\frac{1}{2}\left[I+2\mathrm{Re}(\alpha_0\alpha_1^*)\sigma_x\right]$, and qubits 2 and 3 are in the maximally mixed states with $\rho_2=\rho_3=I/2$, where I and σ_x are the identity and Pauli matrices, respectively. In the first step, the CNOT gate $\mathcal{C}_{21}$ masks the diagonal terms representing the amplitude of qubit 1.

To further obscure the remaining non-diagonal coherent terms, the second step involves introducing an ancillary qubit A, prepared in $|0\rangle$. In the third step, a CNOT gate $\mathcal{C}_{1A}$ is operated on qubits 1 and A (where qubit 1 acts as the control qubit and qubit A is the target qubit). Then the 4-qubit masked state is in the form of

$$|\Phi\rangle_{A123}=\frac{1}{\sqrt{2}}\left[\alpha_0(|0000\rangle+|1111\rangle)+\alpha_1(|0011\rangle+|1100\rangle)\right]. \tag{2}$$

We can see that all the four local states are maximally mixed with $\rho_{A,1,2,3}=I/2$, indicating that the initial quantum information is spreading over quantum correlation in $|\Phi\rangle_{A123}$ and the complete QIM is achieved. The most basic scheme in a 4-qubit system can be formulated as

$$\mathcal{C}_{1A}\mathcal{C}_{21}|0\rangle_A|\gamma\rangle_1|\varphi\rangle_{23}=|\Phi\rangle_{A123}. \tag{3}$$

We choose the polarization degree of freedom (DoF) of photons to carry qubit information for qubit 1. The quantum state to be masked can be substituted with the polarized state of the photon following the correspondences of $|H\rangle\leftrightarrow|0\rangle$ and $|V\rangle\leftrightarrow|1\rangle$, with $|H\rangle$ and $|V\rangle$ indicating the horizontally and vertically linear polarization states of the photon, respectively. Qubit 2 and 3 are also encoded in the polarization DoF, while the ancillary qubit A is encoded in the orbital angular momentum (OAM) DoF with the correspondences of $|+1\rangle\leftrightarrow|0\rangle$ and $|-1\rangle\leftrightarrow|1\rangle$, where $|+1\rangle$ and $|-1\rangle$ refer to the right-handed and the left-handed OAMs of $+\hbar$ and $-\hbar$. Then the 4-qubit masked state can be represented as: $|\Phi\rangle_{A123}=\frac{1}{\sqrt{2}}[\alpha_0(|+1HHH\rangle+|-1VVV\rangle)+\alpha_1(|+1HVV\rangle+|-1VHH\rangle)]$. $|\Phi\rangle_{A123}$ is entangled in three photons with four DoFs, which is called the hyperentangled state.

Here, we show that our scheme includes both complete QIM and unmasking process to reconstruct the masked information, which is quantum teleportation in the 4-qubit system, as shown in Fig. 1. The $|\Phi\rangle_{A123}$ can be unmasked back to qubit 1 by using the inverse operation $(\mathcal{C}_{1A}\mathcal{C}_{21})^\dagger=\mathcal{C}_{21}\mathcal{C}_{1A}$. Similar operations can unmask the quantum information to any of the four parts according to the symmetry of $|\Phi\rangle_{A123}$. For example,

$$\mathcal{C}_{13}\mathcal{C}_{32}|\Phi\rangle_{A123}=|\varphi\rangle_{A1}|0\rangle_2|\gamma\rangle_3 \tag{4}$$

reconstructs the initial state in qubit 3. Furthermore, two arbitrary high-dimensional QIM in the 4-qubit system and an odd high-dimensional QIM version in the tripartite system are shown in Supplementary Note 1.

We indicate that the total masking scenario for a single qubit that we propose for the no-masking theorem can be generalized to quantum information encoded in multipartite systems. In a multipartite systems, if the quantum information is encoded in a direct product state, we can attach a set of masking systems to each qubit to achieve the total QIM. If the quantum information is in an entangled state between different systems, any subsystems will be in a mixed state, which is a mixture of different pure states. Since our QIM scheme applies to any pure state on the Bloch sphere, it also applies to their mixed states. For entangled systems, we can also match the masking systems for each subsystem and perform masking procedures to finalize the total QIM. The total QIM is an unitary process, and the unmasking can be implemented by the inverse operation, which is also a unitary process. So that our scenario can be extended to more multipartite systems.

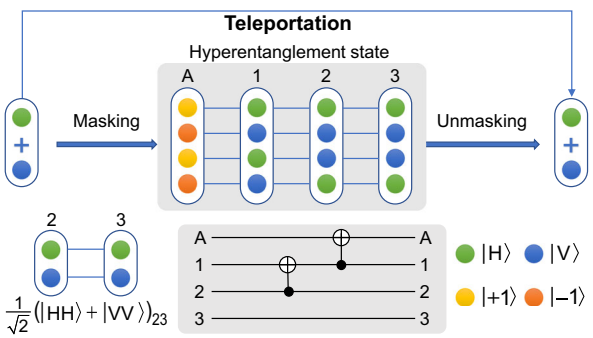

Fig. 1 | The complete QIM process in the 4-qubit system. The two steps of QIM and unmasking can compose the process of quantum teleportation. For the QIM scheme, the initial state which is encoded in the polarization and represented by the green and blue spheres will pass through the two CNOT gates C_{21} and C_{1A} and the initial state will be completely masked in the 4-qubit hyperentangled state. The protocol of unmasking will transmit the initial state to an arbitrary qubit and finish quantum teleportation. The photon pair (photon-2, photon-3) is prepared in the Bell state of $\frac{1}{\sqrt{2}}(|HH\rangle+|VV\rangle)_{23}$.

Complete QIM enables QSS and quantum teleportation

Since masking protocols can be viewed as a basis for QSS[8], our QIM protocol, in which the arbitrary initial state $|\gamma\rangle_1$ can be masked in the minimal Hilbert space with the help of the Bell state $|\varphi\rangle_{23}$ and an ancillary qubit A, can be easily scaled up in multipartite systems with an arbitrary number of participants involved. This enhanced scalability makes QSS implementation more straightforward.

Starting from our masked state $|\Phi\rangle_{A123}$, the second and third steps in our complete QIM scheme can be iterated multiple times to add more qubits involved. The involved CNOT gates are operated on the added qubits and the existing qubits, where the added qubits are the target qubits, and the control qubits can be any qubits of the existing sharing states. To illustrate, let us consider an example of a 6-qubit QSS state. On top of the masked state $|\Phi\rangle_{A123}$, we add two qubits $2'$ and $3'$ prepared in $|0\rangle$ and do the gate operation $\mathcal{C}_{22'}$ and $\mathcal{C}_{33'}$, respectively. Then the 6-qubit QSS state can be written as

$$|\Phi\rangle_{A122'33'} = \frac{1}{\sqrt{2}}\left[\alpha_0(|000000\rangle + |111111\rangle) + \alpha_1(|001111\rangle + |110000\rangle)\right]. \quad (5)$$

Like the complete QIM, the quantum teleportation in quantum information science is another protocol that requires the arbitrariness of qubit state, i.e., the state set covering the whole Bloch sphere. Quantum information schemes and their extensions are widely studied[30–35] and applied in various branches of quantum information from fundamental quantum physics such as loophole-free test of Bell inequality violation[36] to practical applications such as quantum repeater[37] and quantum networks[38–40]. So far, the implementation of quantum teleportation in multiparty systems remains an intriguing and open area of research.

Our work reveals that quantum teleportation can be viewed as a combined process of complete QIM and unmasking. Besides the general unmasking approach above, in the $2^{\otimes 6}$ system given by Eq. (5), the unmasking process can be achieved by some simple Hadamard gates. This process is simpler than the standard paradigm of unmasking. First, the six qubits in the entangled state are divided into two groups $(A, 1)$ and $(2, 2\prime, 3, 3\prime)$. Then, the Hadamard gates are executed on all qubits of the group except for the qubit that receives the initial information, and the qubits without Hadamard gate operation can acquire the initial state by a local operation indicated by a measurement on the computational basis of the qubits of the other group. The details of the unmasking process to an arbitrary subsystem are shown in Supplementary Note 2.

Experiment of complete QIM process

We consider the physical realization of complete QIM. The polarization degree of freedom (DoF) of photons is used to carry qubit information. The quantum state to be masked can be substituted with the polarized state of the photon following the correspondences of $|H\rangle \leftrightarrow |0\rangle$ and $|V\rangle \leftrightarrow |1\rangle$, with $|H\rangle$ and $|V\rangle$ indicating the horizontal and vertical polarizations of the photon, respectively. The experimental setup for arbitrary qubits QIM is shown in Figure 2. The femtosecond (fs) laser with a central wavelength of 390 nm and a repetition rate of 80 MHz pumps successively one single 2 mm-thick β-barium borate (BBO) crystal and standard Kwiat source (i.e., glued two 0.6 mm-thick BBO crystals with perpendicular optical axes) for type-I spontaneous parametric down-conversion (SPDC)[33,41], among which the first photon pair (photon-1 and photon-trigger) is prepared in the product state $|HH\rangle$ pumped by $|V\rangle$, and the second photon pair (photon-2 and photon-3) is the Bell state of $\frac{1}{\sqrt{2}}(|HH\rangle + |VV\rangle)_{23}$ pumped by $|H + V\rangle$, which is regarded as the masking channel. The photon-1 is used to prepare the state that will be masked and its twin photon serves as a trigger to herald the photon-1. Furthermore, we utilize two DoFs of a single photon to encode qubits, namely, the polarization and orbital angular momentum (OAM). The ancillary qubit A is encoded as OAM DoF of the photon-1.

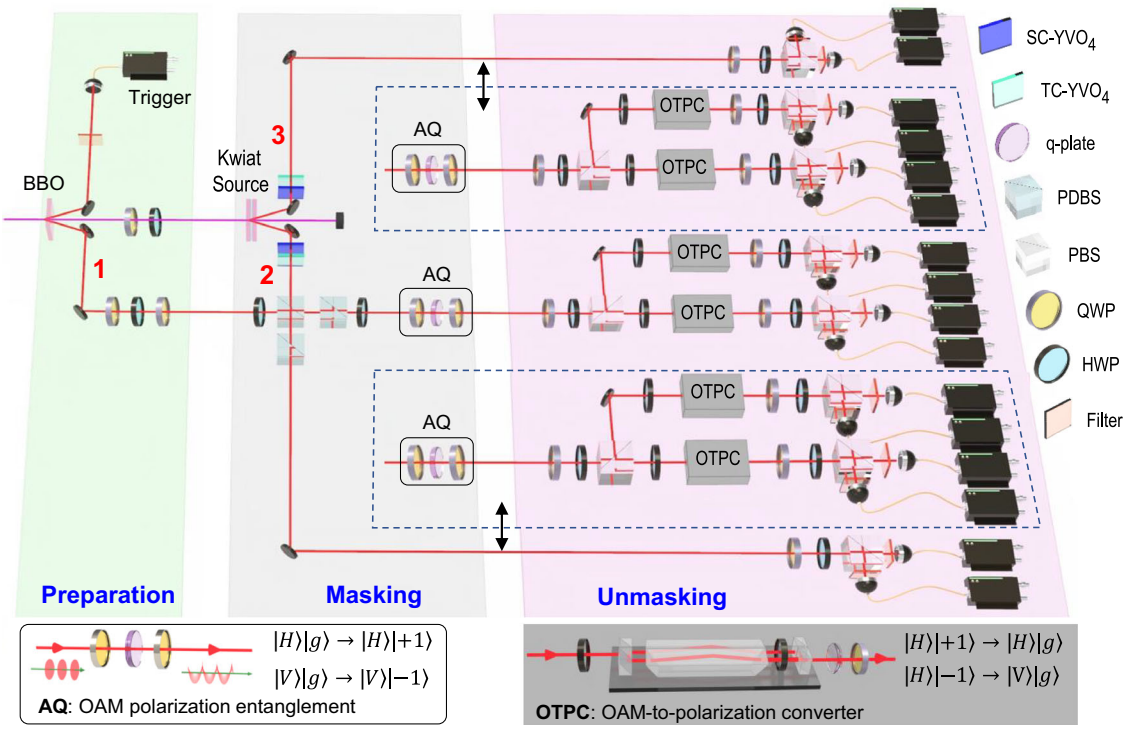

Fig. 2 | Experimental setup to mask an arbitrary qubit and 6-qubit QSS. An ultrafast fs laser beam successively passes through two separate sources. The first one is a single BBO crystal to generate correlated photon pair $|HH\rangle$ and the other one is standard Kwiat source to generate the entangled photon pair $\frac{1}{\sqrt{2}}(|HH\rangle + |VV\rangle)_{23}$. $SC\text{-}YVO_4$ and $TC\text{-}YVO_4$ represent spatial compensation (SC) and temporal compensation (TC) YVO_4 crystals. The polarization CNOT gate is combined by three PDBSs and two HWPs. AQ (auxiliary qubit, see "Methods" for details) is the combination of a q-plate sandwiched by QWPs and prepares the OAM polarization entanglement. OTPC (the OAM-to-polarization converter, see "Methods" for details) is utilized to read the photonic OAM qubit. 6-qubit QSS is realized when the combination of AQ and OTPC acts on both photon-2, photon-3 simultaneously.

To prepare an arbitrary initial state of $|\gamma\rangle_1$ for masking, the photon-1 passes through a half-wave plate (HWP) sandwiched between two quarter-wave plates (QWPs) to achieve an arbitrary unitary polarization rotation, which can map an initial state to any point on the Bloch sphere. In our QIM scenario, the photon-1 undergoes three steps: two CNOT gates and introduction of an ancillary qubit. We apply the first CNOT gate $\mathcal{C}_{21}$ on the photon-1 and photon-2 to mask the diagonal elements of the reduced density matrix of the initial state, where the photon-1 is the target qubit and the photon-2 serves as the control qubit. The CNOT gate with a success probability of 1/9 is composed of the controlled-phase (C-phase) gate and two Hadamard gates (HWP at an angle of 22.5°), as shown in Fig. 2. The C-phase gate is combined by three polarization-dependent beam splitters (PDBSs) with one primary PDBS ($T_H = 1$ and $T_V = 1/3$) and two secondary PDBSs ($T_V = 1$ and $T_H = 1/3$)[42]. In our experiment, the process fidelity of the CNOT operation[43,44] is measured to be $F \in [0.87 \pm 0.02, 0.92 \pm 0.01]$ (see Supplementary Note 3).

The subsequent CNOT gate $\mathcal{C}_{1A}$ is performed on different DoFs of photon-1, namely, polarization and OAM, where polarization DoF is the control qubit and OAM DoF (qubit A) acts as the target qubit, with the correspondences $|+1\rangle \leftrightarrow |0\rangle$ and $|-1\rangle \leftrightarrow |1\rangle$, where $|+1\rangle$ and $|-1\rangle$ refer to the right- and the left-handed OAMs of $+\hbar$ and $-\hbar$. The interfered photon-1 passes through the sandwich structure of a QWP, a q-plate, and a QWP. Such an architecture[45] can easily make $|H\rangle$ photon carry the OAM of $+\hbar$, while $|V\rangle$ photon carries the OAM of $-\hbar$, i.e., $|g\rangle_A|H\rangle_1 \rightarrow |+1\rangle_A|H\rangle_1$ and $|g\rangle_A|V\rangle_1 \rightarrow |-1\rangle_A|V\rangle_1$ (see "Methods" for details), where $|g\rangle$ represents the Gaussian mode of the photon. Then the desired masked 4-qubit hyperentangled state in Eq. (2) can be generated.

After completing the QIM process, one needs to analyze the masked quantum information by the projection measurement of the final state. Polarization qubits 1, 2, and 3 are read out with a standard polarization analyzer, which consists of one HWP, one QWP, and one polarizing beam splitter (PBS). For the qubit A, which is encoded in OAM, a swap gate is employed to transform the OAM information to polarization. Subsequently, another polarization analyzer is used[46]. Finally, the photons are collected by single-mode fibers (SMFs) and sent to the single-photon avalanche detectors for four-fold coincidence counting.

The density matrix of any point on the Bloch sphere can be expressed as a linear superposition of the Pauli matrices[12,47]. To reveal that our work can be completely masked for any qubit on the Bloch sphere, we select 16 initial states (see Supplementary Note 4 for their details). Figure 3a shows all the selected 16 initial states by the two-dimensional 'Map' representation instead of the three-dimensional Bloch sphere, which is prepared by combining QWP, HWP, and QWP (for details, see Supplementary Note 4). We measure the fidelity of the hyperentangled states after QIM for each initial state by representing the density matrix of the hyperentangled state with the identity and Pauli matrices and measuring the corresponding expectation values. The average fidelity of the masking-resulted states is 0.84 ± 0.01 (see Supplementary Note 4 for the fidelities of all the 16 states). The initial state $|H\rangle$ after QIM is the 4-qubit GHZ state. Figure 3b illustrates the measurement results under the computational basis $\{|H\rangle, |V\rangle\}$ to calculate the population and the expectation values of the corresponding entanglement witness operators to calculate the coherence. With the calculated population and coherence, we can easily obtain the fidelity[46]. We present the reduced density matrices of the masked qubits after passing the first and second CNOT gates in Fig. 3c, respectively. The reduced density matrices can be obtained by measuring the expectation of the three Pauli matrices as the measurement operators. After the first CNOT gate, the diagonal terms in the reduced density matrices of the qubits represent the amplitudes that have been masked. For some states, however, the non-diagonal terms representing the coherence terms are still not completely masked. After the second CNOT gate, the reduced density matrix of any single qubit is the maximally mixed state. We calculate the trace distance $T(\rho_i, \rho_j) = \frac{1}{2}\mathrm{Tr}|\rho_i - \rho_j|$[47–50] from the masked qubit to the maximally mixed state with $T \in [0.12 \pm 0.02, 0.03 \pm 0.02]$. This outcome indicates that the information of any single qubit is masked in the 4-qubit hyperentangled state and no information about the initial state can be obtained from any single qubit (see Supplementary Note 4 for details).

Furthermore, building upon the foundation of complete QIM in the 4-qubit system, we further repeat the second and the third steps twice in our QIM scheme to introduce two ancillary qubits 2′ and 3′, which are encoded in the OAM DoF of the photon-2 and photon-3, respectively. Then we perform the CNOT gates $\mathcal{C}_{22'}$ and $\mathcal{C}_{33'}$ via AQ, as shown in Fig. 2. This configuration allows us to prepare the 6-qubit QSS state shown by Eq. (5). We share the six states ($|+\rangle, |-\rangle, |R\rangle, |L\rangle, |H\rangle$, and $|V\rangle$) within the 6-qubit QSS system. Figure 4a presents the measurements of the trace distance from the reduced density matrix of each qubit to the maximally mixed state with the average trace distance of 0.06 ± 0.03. For every qubit, we measure the reduced density matrices by the expectation values of the Pauli matrices. In our proposal, the initial state being shared can be recovered to any qubit by local operations and classical communication. We transfer the six initial states to A, 1, 2, 2′, 3, 3′ qubits, respectively. The data shown in Fig. 4b produces the average teleportation fidelity of 0.85 ± 0.03, which is obtained by the projection measurements on the unmasked qubit. The fidelity of the unmasking process is mainly limited by the first CNOT gate $\mathcal{C}_{21}$. Using deterministic CNOT gate or increasing the visibility of quantum interference can further improve the fidelity. Unmasking process in a 4-qubit system is demonstrated (see Supplementary Note 5 for details).

Conclusion

We have proposed two QIM schemes for the 4-partite system and one for the tripartite system, going beyond no-masking theorem. Experimentally, we have verified the existence of a complete quantum masker in the 4-qubit system and meticulously tested the theoretical predictions, therefore extending the QIM scheme to the multiqubit regime and providing a solid foundation for future verification of high-dimensional quantum information processing[51–59,59,60]. We present an experimental implementation of QIM-based 6-qubit QSS, which also shows the wide application prospect of QIM in the information security. In ref. 15, a stronger version of k-uniform QIM in multipartite systems has been proposed, which requires that the original information remains inaccessible to any subset of subsystems containing k or fewer participants. Our work can be regarded as a 1-uniform QIM, and stronger QIM is expected in the future.

Methods

Introducing the ancillary qubit and $\mathcal{C}_{1A}$

The operations in the second and third steps of QIM could be written as following:

$$\begin{aligned}(\alpha|H\rangle_1 + \beta|V\rangle_1)|g\rangle_1 &\xrightarrow[\text{introducing qubit } A]{\text{second step}} (\alpha|H\rangle_1 + \beta|V\rangle_1)|+1\rangle_A \\ &\xrightarrow[\text{CNOT } \mathcal{C}_{1A}]{\text{third step}} \alpha|H\rangle_1|+1\rangle_A + \beta|V\rangle_1|-1\rangle_A\end{aligned} \tag{6}$$

In the experiment, the introduction of the ancillary qubit A encoded in the orbital angular momentum (OAM) degree of the photon-1 and the implementation of the second CNOT gate $\mathcal{C}_{1A}$ are together implemented by the combination of a q-plate sandwiched by two quarter-wave plates (QWPs) in the following state transfer process:

$$\begin{aligned}(\alpha|H\rangle + \beta|V\rangle)|g\rangle &\xrightarrow{\text{1st QWP}} (\alpha|L\rangle + \beta|R\rangle)|g\rangle \xrightarrow{\text{q-plate}} \alpha|R\rangle|+1\rangle + \beta|L\rangle|-1\rangle \\ &\xrightarrow{\text{2nd QWP}} \alpha|H\rangle|+1\rangle + \beta|V\rangle|-1\rangle.\end{aligned} \tag{7}$$

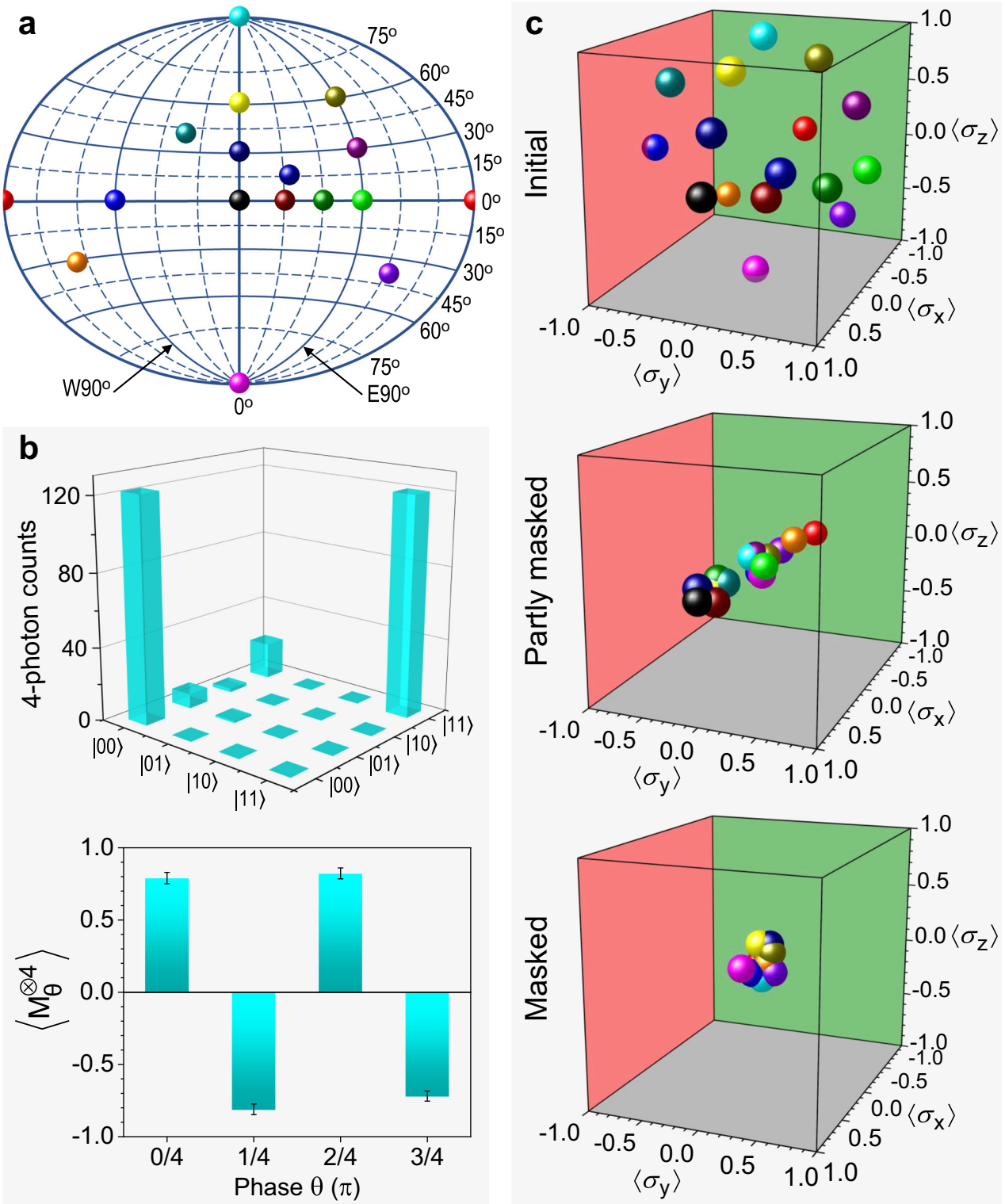

Fig. 3 | Experimental results for the complete QIM of the arbitrary qubit. a The 16 initial states selected on the Bloch sphere, for implementing the QIM experiment, are mapped to the "Map" representation for clarity. **b** For the initial state $|H\rangle$, QIM result is 4-qubit GHZ state. We show the four-photon coincidence counts in $\{|H\rangle, |V\rangle\}$ basis and the expectation values of $M_\theta^{\otimes 4} = (\cos\theta\sigma_x + \sin\theta\sigma_y)^{\otimes 4}$ obtained by the measurement in the basis of $\frac{1}{\sqrt{2}}(|H\rangle \pm e^{i\theta}|V\rangle)$, where $\theta = k\pi/4$ ($k = 0, 1, 2, 3$). The error bar indicates 1 standard deviation (obtained from the Poissonian statistics of the detected four-photon counts). **c** The reduced density matrix of the qubit carrying the initial quantum information at the different stages of the QIM process: before QIM (initial), passing through the first CNOT gate (partially masked), and after QIM (masked).

All the above three processes in expression (7) are deterministic, therefore, the overall operation in the second and third steps of QIM is also in a deterministic manner.

OTPC: the OAM-to-polarization converter

The OAM-to-polarization converter (OTPC) is combined by a HWP, an interferometer, a Q-plate and a QWP as shown in Fig. 2. The interferometer

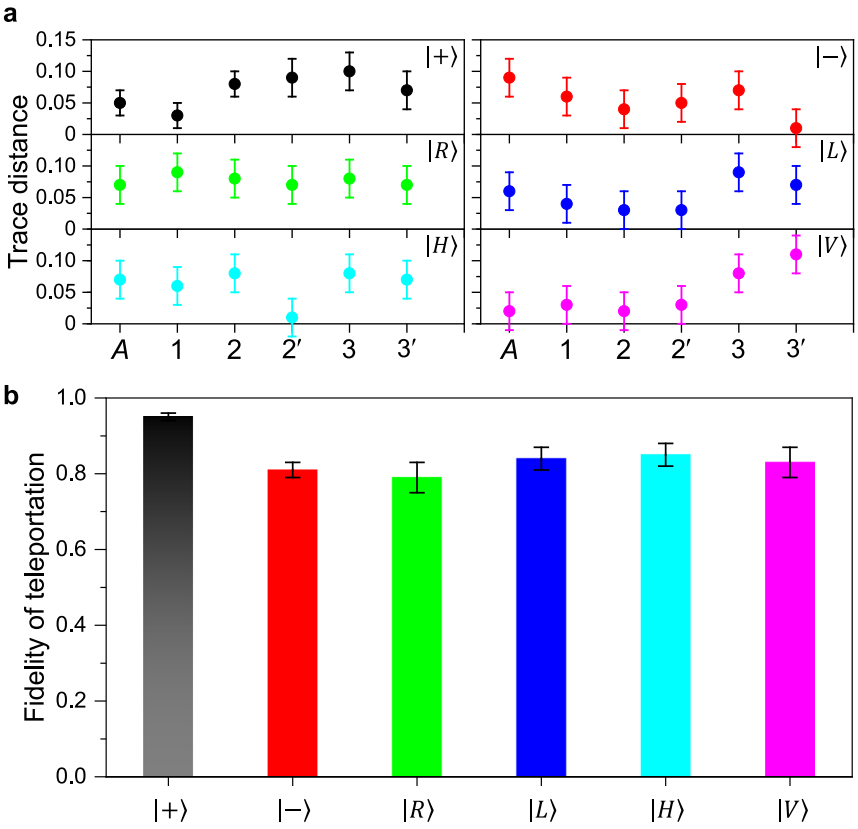

Fig. 4 | QIM enables 6-qubit QSS. a We share six eigenstates of three Pauli matrices into a 6-qubit hyperentangled system and show the trace distance of the reduced density matrix of each qubit from the maximally mixed state. **b** The experimental results of unmasking. We pass each of the six initial states to six different qubits and display the fidelity of each process. The error bar indicates 1 standard deviation (obtained from the Poissonian statistics of the detected four-photon counts).

consists two double-path PBS, two Dove prisms rotated by $\pm\pi/8$ with respect and an HWP. States transform in the interferometer obey the following rules from the input mode to the output mode:

$$\begin{aligned}
&|H\rangle|+1\rangle \to e^{i\pi/4}|V\rangle|-1\rangle,\\
&|H\rangle|-1\rangle \to e^{-i\pi/4}|V\rangle|+1\rangle,\\
&|V\rangle|+1\rangle \to e^{-i\pi/4}|H\rangle|-1\rangle,\\
&|V\rangle|-1\rangle \to e^{i\pi/4}|H\rangle|+1\rangle.
\end{aligned} \tag{8}$$

The transform process is guided by polarization DOF and such a transform is deterministic. Therefore, the state transform in the interferometer is also in a deterministic manner. Then, the state conversion process by our element of OTP could be written step by step in the following form:

$$\begin{aligned}
&|H\rangle\left(\alpha|+1\rangle+\beta|-1\rangle\right)\\
&\xrightarrow{\text{HWP}}\frac{1}{\sqrt{2}}(|H\rangle+|V\rangle)(\alpha|+1\rangle+\beta|-1\rangle),\\
&\xrightarrow{\text{interferometer}}\frac{1}{\sqrt{2}}\left[\alpha e^{i\pi/4}|V\rangle|-1\rangle+\beta e^{-i\pi/4}|V\rangle|+1\rangle+\alpha e^{-i\pi/4}|H\rangle|-1\rangle+\beta e^{i\pi/4}|H\rangle|+1\rangle\right],\\
&=\frac{e^{-i\pi/4}}{\sqrt{2}}\left[\alpha(|H\rangle+i|V\rangle)|-1\rangle+\beta(i|H\rangle+|V\rangle)|+1\rangle\right]\\
&\xrightarrow{\text{Q-plate}}\frac{1}{\sqrt{2}}\left[\alpha(|H\rangle-i|V\rangle)+\beta(-i|H\rangle+|V\rangle)\right]|g\rangle,\\
&\xrightarrow{\text{QWP}}\left(\alpha|H\rangle+\beta|V\rangle\right)|g\rangle.
\end{aligned} \tag{9}$$

As every step is deterministic, the whole conversion process is deterministic in the form:

$$|H\rangle\left(\alpha|+1\rangle+\beta|-1\rangle\right)\to\left(\alpha|H\rangle+\beta|V\rangle\right)|g\rangle. \tag{10}$$

Data availability

All data supporting the findings of this study are available in the main text and Supplementary Information (https://doi.org/10.6084/m9.figshare.28029728.v1). The data are also available from the corresponding authors upon reasonable request.

Received: 21 May 2024; Accepted: 8 January 2025;
Published online: 18 January 2025

References

1. Bennett, C. H. et al. Teleporting an unknown quantum state via dual classical and Einstein-Podolsky-Rosen channels. *Phys. Rev. Lett.* **70**, 1895 (1993).
2. Bouwmeester, D., Weinfurter, H. & Zeilinger, A. Experimental quantum teleportation. *Nature* **390**, 575 (1997).
3. Wootters, W. K. & Zurek, W. H. A single quantum cannot be cloned. *Nature* **299**, 802 (1982).
4. Scarani, V., Iblisdir, S., Gisin, N. & Acín, A. Quantum cloning. *Rev. Mod. Phys.* **77**, 1225 (2005).
5. Pati, A. K. & Braunstein, S. L. Impossibility of deleting an unknown quantum state. *Nature* **404**, 164 (2000).
6. Barnum, H., Caves, C. M., Fuchs, C. A., Jozsa, R. & Schumacher, B. Noncommuting mixed states cannot be broadcast. *Phys. Rev. Lett.* **76**, 2818 (1996).
7. Braunstein, S. L. & Pati, A. K. Quantum information cannot be completely hidden in correlations: Implications for the black-hole information paradox. *Phys. Rev. Lett.* **98**, 080502 (2007).
8. Modi, K., Pati, A. K., Sen, A. & Sen, U. Masking quantum information is impossible. *Phys. Rev. Lett.* **120**, 230501 (2018).
9. Zhu, H. Hiding and masking quantum information in complex and real quantum mechanics. *Phys. Rev. Res.* **3**, 033176 (2021).
10. Liang, X. B., Li, B., Fei, S. M. & Fan, H. Impossibility of masking a set of quantum states of nonzero measure. *Phys. Rev. A* **101**, 042321 (2020).

11. Liang, X. B., Li, B. & Fei, S. M. Complete characterization of qubit masking. *Phys. Rev. A* **100**, 030304(R) (2019).
12. Liu, Z. H. et al. Photonic implementation of quantum information masking. *Phys. Rev. Lett.* **126**, 170505 (2021).
13. Zhang, R. Q. et al. Experimental masking of real quantum states. *Phys. Rev. Appl.* **16**, 024052 (2021).
14. Li, M. S. & Wang, Y. L. Masking quantum information in multipartite scenario. *Phys. Rev. A* **98**, 062306 (2018).
15. Shi, F., Li, M. S., Chen, L. & Zhang, X. *k*-uniform quantum information masking. *Phys. Rev. A* **104**, 032601 (2021).
16. Tian, G., Yu, S., Gao, F., Wen, Q. & Oh, C. H. Local discrimination of four or more maximally entangled states. *Phys. Rev. A* **91**, 052314 (2015).
17. Lo, H. K. & Chau, H. F. Is quantum bit commitment really possible? *Phys. Rev. Lett.* **78**, 3410 (1997).
18. Mayers, D. Unconditionally secure quantum bit commitment is impossible. *Phys. Rev. Lett.* **78**, 3414 (1997).
19. Hillery, M., Bužek, V. & Berthiaume, A. Quantum secret sharing. *Phys. Rev. A* **59**, 1829 (1999).
20. Lie, S. H. & Jeong, H. Randomness cost of masking quantum information and the information conservation law. *Phys. Rev. A* **101**, 052322 (2020).
21. Cleve, R., Gottesman, D. & Lo, H. K. How to share a quantum secret. *Phys. Rev. Lett.* **83**, 648 (1999).
22. Karlsson, A., Koashi, M. & Imoto, N. Quantum entanglement for secret sharing and secret splitting. *Phys. Rev. A* **59**, 162 (1999).
23. Tittel, W., Zbinden, H. & Gisin, N. Experimental demonstration of quantum secret sharing. *Phys. Rev. A* **63**, 042301 (2001).
24. Chen, Y. A. et al. Experimental quantum secret sharing and third-man quantum cryptography. *Phys. Rev. Lett.* **95**, 200502 (2005).
25. Gaertner, S., Kurtsiefer, C., Bourennane, M. & Weinfurter, H. Experimental demonstration of four-party quantum secret sharing. *Phys. Rev. Lett.* **98**, 020503 (2007).
26. Zhou, Y. et al. Quantum secret sharing among four players using multipartite bound entanglement of an optical field. *Phys. Rev. Lett.* **121**, 150502 (2018).
27. Lance, A. M., Symul, T., Bowen, W. P., Sanders, B. C. & Lam, P. K. Tripartite quantum state sharing. *Phys. Rev. Lett.* **92**, 177903 (2004).
28. Lu, H. Secret sharing of a quantum state. *Phys. Rev. Lett.* **117**, 030501 (2016).
29. Bell, B. A. et al. Experimental demonstration of graph-state quantum secret sharing. *Nat. Commun.* **5**, 5480 (2014).
30. Furusawa, A. et al. Unconditional quantum teleportation. *Science* **282**, 706 (1998).
31. Marcikic, I., de Riedmatten, H., Tittel, W., Zbinden, H. & Gisin, N. Long-distance teleportation of qubits at telecommunication wavelengths. *Nature* **421**, 509 (2003).
32. Zhang, Q. et al. Experimental quantum teleportation of a two-qubit composite system. *Nat. Phys.* **2**, 678 (2006).
33. Wang, X. L. et al. Quantum teleportation of multiple degrees of freedom of a single photon. *Nature* **518**, 516 (2015).
34. Pirandola, S., Eisert, J., Weedbrook, C., Furusawa, A. & Braunstein, S. L. Advances in quantum teleportation. *Nat. Photonics* **9**, 641 (2015).
35. Ren, J. G. et al. Ground-to-satellite quantum teleportation. *Nature* **549**, 70 (2017).
36. Hensen, B. et al. Loophole-free Bell inequality violation using electron spins separated by 1.3 kilometres. *Nature* **526**, 682 (2015).
37. Sangouard, N., Simon, C., de Riedmatten, H. & Gisin, N. Quantum repeaters based on atomic ensembles and linear optics. *Rev. Mod. Phys.* **83**, 33 (2011).
38. Duan, L. M. & Monroe, C. Colloquium: quantum networks with trapped ions. *Rev. Mod. Phys.* **82**, 1209 (2010).
39. Wehner, S., Elkouss, D. & Hanson, R. Quantum internet: a vision for the road ahead. *Science* **362**, 303 (2018).
40. Hermans, S. L. N. et al. Qubit teleportation between non-neighbouring nodes in a quantum network. *Nature* **605**, 663 (2022).
41. Barreiro, J. T., Langford, N. K., Peters, N. A. & Kwiat, P. G. Generation of hyperentangled photon pairs. *Phys. Rev. Lett.* **95**, 260501 (2005).
42. Lu, H. et al. Experimental realization of a concatenated Greenberger-Horne-Zeilinger state for macroscopic quantum superpositions. *Nat. Photon.* **8**, 364 (2014).
43. Langford, N. K. et al. Demonstration of a simple entangling optical gate and its use in bell-state analysis. *Phys. Rev. Lett.* **95**, 210504 (2005).
44. Hofmann, H. F. Complementary classical fidelities as an efficient criterion for the evaluation of experimentally realized quantum operations. *Phys. Rev. Lett.* **94**, 160504 (2005).
45. Marrucci, L., Manzo, C. & Paparo, D. Optical spin-to-orbital angular momentum conversion in inhomogeneous anisotropic media. *Phys. Rev. Lett.* **96**, 163905 (2006).
46. Wang, X. L. et al. 18-Qubit entanglement with six photons' three degrees of freedom. *Phys. Rev. Lett.* **120**, 260502 (2018).
47. Nielsen, M. A. & Chuang, I. L. *Quantum Computation and Quantum Information: 10th Anniversary Edition*. (Cambridge University Press, Cambridge, England, 2010).
48. Breuer, H. P., Laine, E. M. & Piilo, J. Measure for the degree of non-markovian behavior of quantum processes in open systems. *Phys. Rev. Lett.* **103**, 210401 (2009).
49. Xiao, L. et al. Observation of critical phenomena in parity-time-symmetric quantum dynamics. *Phys. Rev. Lett.* **123**, 230401 (2019).
50. Wang, Y. T. et al. Experimental investigation of state distinguishability in parity-time symmetric quantum dynamics. *Phys. Rev. Lett.* **124**, 230402 (2020).
51. Luo, Y. H. et al. Quantum teleportation in high dimensions. *Phys. Rev. Lett.* **123**, 070505 (2019).
52. Hu, X. M. et al. Experimental high-dimensional quantum teleportation. *Phys. Rev. Lett.* **125**, 230501 (2020).
53. Sephton, B. et al. Quantum transport of high-dimensional spatial information with a nonlinear detector. *Nat. Commun.* **14**, 8243 (2023).
54. Qiu, X. D., Guo, H. X. & Chen, L. X. Remote transport of high-dimensional orbital angular momentum states and ghost images via spatial-mode-engineered frequency conversion. *Nat. Commun.* **14**, 8244 (2023).
55. Dada, A. C., Leach, J., Buller, G. S., Padgett, M. J. & Andersson, E. Experimental high-dimensional two-photon entanglement and violations of generalized Bell inequalities. *Nat. Phys.* **7**, 677 (2011).
56. Zeng, Q., Wang, B., Li, P. & Zhang, X. Experimental high-dimensional Einstein-Podolsky-Rosen steering. *Phys. Rev. Lett.* **120**, 030401 (2018).
57. Erhard, M., Krenn, M. & Zeilinger, A. Advances in high-dimensional quantum entanglement. *Nat. Rev. Phys.* **2**, 365 (2020).
58. Hu, X. M. et al. Efficient generation of high-dimensional entanglement through multipath down-conversion. *Phys. Rev. Lett.* **125**, 090503 (2020).
59. Hiekkamäki, M. & Fickler, R. High-dimensional two-photon interference effects in spatial modes. *Phys. Rev. Lett.* **126**, 123601 (2021).
60. Designolle, S. et al. Genuine high-dimensional quantum steering. *Phys. Rev. Lett.* **126**, 200404 (2021).

Acknowledgements

This work was supported by National Natural Science Foundation of China (Nos. 12234009, 12274215); National Key Research and Development Program of China (Nos. 2019YFA0308700, 2020YFA0309500); Innovation Program for Quantum Science and Technology (No. 2021ZD0301400); Program for Innovative Talents and Entrepreneurs in Jiangsu; Key Research and Development Program of Guangdong Province (No. 2020B0303010001). J.L.C. was supported by National Natural Science

Foundations of China (Nos. 12275136, 12075001) and Fundamental Research Funds for the Central Universities (No. 3072022TS2503).

Author contributions

Hui-Tian Wang, Xi-Lin Wang, Fu-Lin Zhang, and Jing-Ling Chen designed the research and supervised the project; Zhi-Feng Liu, Xi-Lin Wang, and Hui-Tian Wang dominantly performed the experiment and implemented the numerics; Zi-Mo Cheng, Wen-Zheng Zhu, Hao Li, Pei Wan, Shu-Tian Xue, Yan-Chao Lou, Chao Chen, and Zhi-Cheng Ren assisted the experiment; Wei-Min Shang, Jia-Min Xu, He Lu, Fu-Lin Zhang, and Jing-Ling Chen dominantly implemented the theory; Zhi-Feng Liu, Jing-Ling Chen, He Lu, Xi-Lin Wang and Hui-Tian Wang analyzed the results and wrote the manuscript; all authors discussed the results and reviewed the manuscript.

Competing interests

The authors declare no competing interests.

Additional information

Supplementary information The online version contains supplementary material available at https://doi.org/10.1038/s42005-025-01942-4.

Correspondence and requests for materials should be addressed to Fu-Lin Zhang, Jing-Ling Chen or Xi-Lin Wang.

Peer review information *Communications Physics* thanks Arun Kumar Pati and the other, anonymous, reviewer(s) for their contribution to the peer review of this work. A peer review file is available.